Title

Human Mesenchymal Stem Cells efficiently manage oxidative stress

Authors

Araceli Valle-Prieto and Paulette A. Conget

Contact information and affiliation of authors

Araceli Valle-Prieto

address: Av Las Condes 12,438. Lo Barnechea. Santiago. Chile

telephone: (562) 327 9302

FAX: (562) 299 9306

e-mail: maricelivp@yahoo.com

affiliations:

- Instituto de Ciencias, Facultad de Medicina Clinica Alemana Universidad del Desarrollo. Santiago. Chile.
- Programa Doctorado en Farmacologia, Facultad de Ciencias Quimicas y Farmaceuticas. Universidad de Chile. Santiago. Chile.

Paulette A. Conget

address: Av Las Condes 12,438. Lo Barnechea. Santiago. Chile

telephone: (562) 327 9157

FAX: (562) 299 9306

e-mail: pconget@udd.cl

affiliation:

- Instituto de Ciencias, Facultad de Medicina Clinica Alemana Universidad del Desarrollo. Santiago. Chile.

Running title

hMSC efficiently manage oxidative stress

Corresponding author

Paulette A. Conget, PhD

address: Av Las Condes 12,438. Lo Barnechea. Santiago. Chile

telephone: (562) 327 9157

FAX: (562) 299 9306

e-mail: pconget@udd.cl

List of Abbreviations

hMSCs, human mesenchymal stem cells; hFibs, human skin fibroblasts, OS, oxidative stress; ROS, reactive oxygen species; RNS, reactive nitrogen species; H_2O_2, oxygen peroxide; SNAP, S-nitroso-N-acetylpenicillamine; SIN-1, 3-morpholinosydnonimine hydrochloride; SOD1, cytosolic superoxide dismutase; SOD2, mitochondrial superoxide dismutase; CAT, catalase; GPX1, glutathione peroxidase 1, GSx, total glutathione.

Abstract

The transplantation of Mesenchymal Stem Cells (MSCs) proves to be useful to treat pathologies in which tissue damage is linked to oxidative stress (OS). The aim of our work was to evaluate whether primary human MSCs manage OS. For this, i*n vitro* we assessed: i) cell viability of hMSCs exposed to increasing concentrations of reactive oxygen species (ROS, source H_2O_2), reactive nitrogen species (RNS, source SNAP) or both (ROS and RNS, source SIN-1); ii) intracellular level of reactive species in hMSCs exposed to ROS and RNS; iii) basal gene expression and activity of superoxide dismutases, catalase and glutathione peroxidase of hMSCs; iv) basal glutathione (GSx) level of hMSCs; and v) cell viability of GSx-depleted hMSCs exposed to ROS and/or RNS. Results showed that hMSCs have a high resistance to OS-induced death, which correlates with low levels of intracellular reactive species, constitutive expression of enzymes required to manage OS and high levels of GSx. When hMSCs were depleted of GSx they lose their capacity to manage OS. Thus, *in vitro* hMSCs are able to scavenge ROS and RNS and efficiently manage OS. Whereas this potential is maintained *in vivo*, hMSCs could also contribute to tissue regeneration limiting OS-induced tissue damage.

Introduction

Stem cells are characterized by their ability to self renew and their potential to differentiate, at least, into one type of mature cell. Stem cells are classified as embryonic (ESCs) or adult (ASCs) depending on the developmental stage of their source. ESCs are derived from the inner cell mass of the blastocyst (day 5 of human embryonic development) and are considered pluripotent because they give rise to all cell types that constitute an organism. ASCs can be obtained from various organs and tissues such as: skin, liver, intestines, heart, kidney and bone marrow [1]. Mesenchymal Stem Cells, also referred as Multipotent Stromal Cells (MSCs), is a type of ASCs found in the bone marrow together with hematopoietic stem cells (HSCs) [2, 3]. MSCs are considered multipotent because they can give rise to a wide repertoire of mesodermal mature cells like adipocytes, chondrocytes, osteocytes and myocytes. They can also generate cells of other lineages like neumocytes [4], hepatocytes [5], neurons [6] and insulin-producing cells [7]. Human MSCs (hMSCs) appear as an ideal tool for cell therapy. They are easily isolated, can be expanded *ex vivo* and have the potential to differentiate into mature cells of different lineages. Moreover, hMSCs have immunoregulatories properties and they are hypoimmunogenic [8]. In effect, transplanted hMSCs are not rejected even in a non-histocompatible recipient [9]. The administration of hMSCs has proved beneficial effects in patients with Osteogenesis Imperfecta [10], Dystrophic Epidermolysis Bullosa [11] Graft versus Host Disease [12] and Acute Myocardial Infarction [13]. In animal models, MSC transplantation allowed the recovery of motor and sensory functions after cerebral stroke [14]. Also, reverts hyperglycemia and prevents nephropathy in diabetic mice [15, 16]. The therapeutic effects of transplanted MSCs have been associated to the following mechanisms: i) differentiation to parenchymal cell; ii) production of trophic factors that promote proliferation and differentiation of local progenitor cells; iii) neovascularization; and iv) immunomodulation [17].

hMSCs are resistant to *ex vivo* culture and ionizing radiation, two conditions that generate a strong oxidative stress (OS) [18, 19]. In view of these observations together with the fact that hMSCs prove to be useful in the treatment of pathologies in which tissue damage is linked to OS, we hypothesize that hMSCs efficiently manage OS. To test our hypothesis we performed *in vitro* studies in order to determine: i) hMSC susceptibility to OS-induced death; ii) the correlation of this susceptibility to intracellular levels of reactive species; iii) hMSC gene expression and activity of enzymes involved in the elimination of reactive species like cytosolic superoxide dismutase (SOD1), mitochondrial superoxide dismutase (SOD2), catalase (CAT) and glutathione peroxidase 1 (GPX1); iv) hMSC basal level of glutathione (GSx), and v) hMSC susceptibility to OS-induced death when they were GSx-depleted. Data for hMSCs were compared with results obtained for INS-1 cells, an OS-sensitive cell model and for human skin fibroblasts (hFibs), an OS-resistant cell model [20].

Materials and Methods

Isolation, culture and characterization of hMSCs

hMSCs were isolated from heparinized bone marrow samples that were discarded because they were unused for allogeneic transplantation procedures. Cells were cultured in alpha-MEM (Sigma, St. Louis, MO, USA) supplemented with 10% (v/v) fetal bovine serum (FBS, Hyclone, Logan, UT, USA) and 40 mg/mL gentamicin (Calbiochem, San Diego, CA, USA), and maintained at 37°C in a humidified atmosphere containing 5% (v/v) CO_2 [2]. One week later, when the monolayer of adherent cells reached almost confluence, cells were trypsinized, washed and subcultured at a density of 7,000 cells/cm^2. Adherent cells were characterized according to their immunophenotype and to their differentiation potential to adipogenic, chondrogenic and osteogenic lineages [2, 3]. In the

later case, cells were cultured in the presence of differentiation stimuli and then examined for the presence of lipid droplets, proteoglycan secretion and matrix mineralization, respectively.

Isolation and culture of hFibs

To establish hFibs cultures leftover materials obtained from skin biopsies of normal individuals were utilized. Skin pieces were seeded in plastic culture dishes and covered with alpha-MEM supplemented with 10% (v/v) FBS, 40 mg/mL gentamicin and 0.2 mg/mL amphotericin B (Gibco, Grand Island, NY, USA), and maintained at 37°C in a humid atmosphere containing 5% (v/v) CO_2. Twice a week, non-adherent skin pieces were eliminated and half of the culture medium was renewed. The adherent skin pieces were discarded when cells were confluent around them. hFibs thus obtained were trypsinized, washed and subcultured at a density of 7,000 cells/cm^2.

Culture of INS-1 cells

Cells referred as INS-1 correspond to INS-1 clone 832/13 cells. They were cultivated in RPMI 1640, 10% (v/v) FBS, 10 mM Hepes, 1 mM pyruvate, 50 uM beta-mercaptoethanol, 100 U/mL penicillin and 100 mg/mL streptomycin, as previously described [21].

Cytotoxicity assay

Twenty four hours before the assay, hMSCs and hFibs were seeded at 25,000 cells/cm^2 and INS-1 cells at a 60,000 cells/cm^2. Then, culture medium was supplemented with: H_2O_2 (Sigma, St. Louis, MO, USA), S-nitroso-N-acetylpenicillamine (SNAP, Sigma, St. Louis, MO, USA) or 3-morpholinosydnonimine hydrochloride (SIN-1, Sigma, St. Louis, MO, USA). Eighteen hours later, non-adherent cells were discarded and adherent cells were stained with 0.2% (w/v) crystal violet dissolved in 10% methanol (v/v). After four washes, cell-

incorporated dye was solubilized by 5 minutes incubation in 50% (v/v) methanol, 50% (v/v) NaH2PO4 0.1 M, pH 4.5. Aliquots of 150 uL were transferred to a 96-plate well and the absorbance at 570 nm (A570) was measured in a microplate reader (Sunrise, Tecan, Austria). Viability corresponded to the ratio between A570 in the presence of reactive specie source and A570 in the absence of it x 100. Lethal concentration 50 (LC_{50}) was calculated by lineal regression analysis of reactive specie source concentration vs. viability plots [22].

Assessment of intracellular reactive specie level

hMSCs and hFibs were seeded at 25,000 cells/cm^2 and INS-1 cells at 60,000 cells/cm^2. One day later, the cells were incubated with 0.75 mM SIN-1 for 1 hour. Then, the cells were washed with phosphate buffer saline (PBS) and incubated with 5 uM dihydrorhodamine 123 (DHR, Calbiochem, San Diego, CA, USA) for 1 hour. Samples were examined in a CyAn ADP flow cytometer (488 and 633 nm) (Dako, Carpinteria, CA, USA) and data were analyzed with Summit 4.3 software (Dako, Carpintería, CA, USA). Net fluorescence intensity (NFI) was calculated as the quotient between the mean fluorescence intensity of the cells stained with DHR and its autofluorescence (without DHR). The level of intracellular reactive species in cells submitted to OS was expressed as the ratio between the NFI of the sample (exposed to SIN-1) and the NFI of the control (unexposed).

Real-time RT-PCR for SOD1, SOD2, CAT and GPX1

Total RNA of hMSCs and hFibs was extracted using TRIzol reagent (Invitrogen, Carlsbad, CA, USA) following the manufacturer's instructions. Remnant genomic DNA was degraded using DNAasa I (Invitrogen, Carlsbad, CA, USA). RNA was quantified spectrophotometrically at 260 nm. For RT reaction, 1 ug of total RNA, 200 U M-MLV

reverse transcriptase (Promega, Madison, WI, USA) and 300 pmoles oligo(dT) primer in 25 uL of total reaction mixture were used. The reaction was conducted following the manufacturer's instructions of the enzyme. Real-time PCR was performed using 2 uL RT reaction, 0.5 uM each of the specific primers (Table 1) and LightCycler-DNA Master SYBR Green I kit (Roche, Indianapolis, IN, USA) in a LigthCycler instrument (Roche, Indianapolis, IN, USA). The amplicons were characterized according to their melting temperature in the later instrument and to their size by agarose gel electrophoresis stained with ethidium bromide. The gene expression level of each enzyme was standardized against *GAPDH* and compared among cells by the comparative Ct method [26].

Enzymatic activity assay for SOD, CAT and GPX1

hMSCs and hFibs were seeded at 7,000 cells/cm^2 and INS-1 cells at a 35,000 cells/cm^2. When the cells became 80-90% confluent they were collected using a rubber policeman and intracellular proteins were release by 3 freeze/thaw cycles (liquid nitrogen/thermoregulated bath at 37°C). Total protein concentration was determined using the BCA1 kit (Sigma, St. Louis, MO, USA) following the manufacturer's instructions.

For SOD activity quantification, 1 mL of SOD lysis buffer (20 mM Hepes, 1 mM EGTA, 210 mM mannitol, 70 mM sucrose and 0.1% (v/v) Triton X-100; pH 7.2) was used to extract proteins from 1 million of cells. SOD activity was measured using the Superoxide Dismutase Assay II kit (Calbiochem, San Diego, CA, USA). This spectrophotometric method allows the quantification of SOD activity in a range of 0.025-0.250 units/mL (1 unit is defined as the amount of enzyme necessary to dismutate 50% of superoxide species).

For CAT activity quantification, 1 mL of CAT lysis buffer (50 mM potassium, 1 mM EDTA and 0.1% (v/v) Triton X-100; pH 7.0) was used to extract proteins from 1 million of cells. CAT activity was measured using the Catalase Assay kit (Calbiochem, San Diego, CA,

USA). This spectrophotometric method allows the quantification of CAT activity in a range of 0.25-4.00 nmol/min/mL (formaldehyde produced).

For GPX1 activity quantification, 1 mL of GPX1 lysis buffer (50 mM Tris-HCl, 5 mM EDTA and 1 mM DTT; pH 7.5) was used to extract proteins from 1 million of cells. GPX1 activity was measured using the Glutathione Peroxides' Assay kit (Calbiochem, San Diego, CA, USA). This spectrophotometric method allows the quantification of GPX1 activity in a range 50-344 nmol/min/mL (NADPH oxidized).

Enzymatic activity data were standardized against total protein amount and expressed as U/mg for SOD, and nmol/min/mg for CAT and for GPX1.

Quantification of GSx

It has been reported that culture media supplements, particularly beta-mercaptoethanol, modified the intracellular levels of glutathione [27]. For this reason, when the basal levels of GSx was assessed all tested cells were cultivated in alpha-MEM 10% (v/v) FBS containing 40 mg/mL gentamicin. hMSCs and hFibs were seeded at 25,000 cells/cm^2 and INS-1 cells at a 60,000 cells/cm^2. Twenty four hours later cells were collected by tripsinization and washed 2 times with PBS. The cells were lysed with 50 uL 0.4% (v/v) Triton X-100 and 3 freeze/thaw cycles (liquid nitrogen/thermoregulated bath at 37ºC). Immediately, 50 uL of ice-cold 5% (w/v) sulfosalicylic acid (Sigma, St. Louis, MO, USA) was added and the mix was incubated for 15 minutes on ice. The cell lysate was centrifuged at 10,000 x g for 2 minutes at 4ºC. The supernatant was stored at -80ºC until GSx quantification. For this, we used the protocol described by Tietze [28] adjusted for microplates [29]. Briefly, to each well plate 10 uL cell lysate were mixtured with 150 uL 100 mM phosphate buffer pH 7.4 containing 3.9 mM EDTA, 15 ug DTNB (Sigma, St. Louis, MO, USA) and 24 mU glutathione reductase (Sigma, St. Louis, MO, USA). Then, 50 uL of phosphate buffer containing 8 ug NADPH (Sigma, St. Louis, MO, USA) was added. The

formation of TNB was detected spectrophotometrically at 405 nm every 12 seconds for 2 minutes, using a plate reader instrument (Tecan, Salzburg, Austria). The concentration of GSx was calculated through interpolation in the calibration curve made with different concentrations of reduced glutathione (Sigma, St. Louis, MO, USA) prepared in phosphate buffer with 0.2% (v/v) Triton X-100 and 2.5% (w/v) acid sulfosalicylic. Results were standardized to 1 million cells and data were expressed as nmoles GSx/million cells.

GSx depletion

hMSCs were seeded at 25,000 cells/cm^2. After 24 hours, 150 uM butyrate sulfoximine (BSO, Sigma, St. Louis, MO, USA) and 1 mM diethilmaleate (DEM, Sigma, St. Louis, MO, USA) were added to the culture medium. One hour later, cytotoxic assays were performed.

Statistical analysis

Results were expressed as mean ± standard error of the mean. Differences between two groups were analyzed by Student *t* test and the differences between more than two groups were analyzed by oneway ANOVA and Newman-Keuls Multiple Comparison as a post-test using GraphPad Prism 5.0 software. We worked with 95% confidence and statistical significance was proved when $p < 0.05$.

Results

High resistance of hMSCs to OS-induced death

hMSCs were cultured for 18 hours with increasing concentrations of ROS (source H_2O_2), RNS (source SNAP) or both (source SIN-1). Then, hMSCs survival (viability) was evaluated by staining of adherent cells with crystal violet. Figure 1 shows raw data of a cytotoxicity assay and LC_{50} interpolation in the reactive specie source concentration vs.

viability plot. As seen in Table 2, LC_{50} values determined for hMSCs were significantly higher than that determined for INS-1 cells, the OS-sensitive cell model. There were no statistical differences when comparing LC_{50} values obtained for hMSCs versus these obtained for hFibs, the OS-resistant cell model. Showing that hMSCs are highly resistant to OS-induced death.

Low intracellular levels of reactive species in hMSCs exposed to OS

In order to determine the levels of intracellular reactive species in hMSCs exposed to OS, cells were incubated for 1 hour in alpha-MEM 10% (v/v) FBS supplemented or not with 0.75 mM SIN-1. The levels of intracellular reactive species were determined by flow cytometry after staining with DHR. The DHR is a cell-permeable fluorogenic probe that difuse within the cell, where it reacts with peroxide and peroxynitrite generating rhodamine. In turn, this is a water-soluble compound and therefore is trapped in the cells. Thus, after staining, the fluorescence emitted by each cell is directly proportional to the amount of intracellular reactive species. As shown in Figure 2, hMSCs exposed to ROS and RNS presented intracellular levels of reactive species significantly lower than those of INS-1 cells ($p < 0.0015$), and similar to those of hFibs (no statistical significance). Therefore, hMSCs efficiently scavenge reactive species.

Gene expression and enzymatic activity of SOD1, SOD2, CAT and GPX1 in hMSCs

Expression of the genes coding for enzymes involved in the elimination of reactive species (*SOD1, SOD2, CAT* and *GPX1*) was assessed by real-time RT-PCR. For all tested genes a single peak at the predictable theoretical values was obtained when amplicon melting point analyses were performed (Figure 3 and Table 1). Also, a single band of the expected size was observed when PCR products were gel electrophoresed (data not shown). Hence, hMSCs express *SOD1, SOD2, CAT* and *GPX1* constitutively. Furthermore,

quantitative analysis showed that hMSCs express *SOD1, SOD2, CAT* and *GPX-1* at similar levels to those expressed in hFibs (no statistical significance, Table 3). Accordingly, the activity of SOD, CAT and GPX1 was similar between hMSCs and hFibs (no statistical significance, Figure 4). However, hMSCs presented a basal activity of these enzymes significantly higher than that of INS-1 cells (in the limit of statistical significance for SOD; $p < 0.005$ for CAT and GPX1; Figure 4).

High levels of GSx in hMSCs

As seen in Figure 5, the basal level of GSx was significantly higher in hMSCs than in INS-1 cells ($p < 0.05$). By another hand, both hMSCs and hFibs presented the same basal levels of GSx (no statistical significance).

Data obtained for INS-1 cells, an OS-sensitive cell model, and hFibs, an OS-resistant cell model, suggest a correlation between the presence and extent of the cellular mechanisms required to scavenge reactive species and cell susceptibility to OS-induced death. Thus, the high resistance of hMSCs to OS-induced death can be considered as a functional prove of they substantial antioxidant defense potential.

High resistance of hMSCs to OS-induced death depends on GSx availability.

As expected, the exposure of hMSCs to BSO and DEM resulted in a significant decrease of the intracellular level of GSx (> 80%). Observed depletion lasted for 11 hours after BSO and DEM withdraw. As seen in Figure 6, GSx-depleted hMSCs showed LC_{50} values for H_2O_2, SNAP and SIN-1 significantly lower than that of hMSCs ($p < 0.05$) and similar to that of INS-1 cells (no statistical significance). Hence, GSx-depleted hMSCs completely lose their ability to highly resist to OS-induced death, becoming as sensible as INS-1 cells.

Discussion

hMSC transplantation has been proved as a therapeutic strategy in individuals with OS-related diseases such as Acute Myocardial Infarction [13], Cerebral Ischemia [14] and Diabetes [15, 16]. However, there is scarce information related to the potential of hMSCs to manage OS. In the present work we show that hMSCs are highly resistant to OS-induced death (Table 1). This low susceptibility to the harmful effect of reactive species correlates with the ability of hMSCs to effectively scavenge peroxide and peroxynitrite (Figure 2). In turn, the later associates with the constitutive expression and activity of SOD1, SOD2, CAT and GPX1 enzymes (Figures 3 and 4), and depends on the high level of intracellular GSx (Figures 5 and 6) detected in hMSCs. Furthermore, we found that hMSCs expressed constitutively and at a high level methionine sulfoxide reductase A (data not shown), an enzyme crucial for the repair of oxidized proteins and for the recovery of methionine residues that act as scavengers of oxidants [30]. Also, it has been reported that hMSCs express the enzymes required for DNA repair [31]. Hence, hMSCs possess the main enzymatic and non-enzymatic mechanisms to detoxify reactive species and to correct oxidative damage of proteome and genome, guarantying an efficiently management of OS. Our biochemical results were not without precedent because it has been published that rat MSCs, the immortalized cell line hMSC-TERT and human bone marrow stromal cells cultured in the presence of ascorbate, express active SOD1, SOD2, CAT, GPXs and thioredoxin reductases [32, 33]. However, up to our knowledge, there were no evidences for the high resistance of hMSCs to OS-induced death or for the main role played by GSx on it.

Appropriate intracellular levels of ROS play a key function in regulating the self-renew and differentiation potential of HSCs [34]. However, when they become excessive, oxidative damage accumulates and results in senescence, apoptosis and/or transformation of the cells. Here we show that the maintenance of the redox status of hMSCs is ensured by a

machinery complex and abundant. Therefore, an accurate management of OS seems to be a critical feature for all stem cells. A fact that takes more relevance when considering that *in vivo* stem cells have a long lifespan and are exposed to OS for long periods of time.

Using rat MSCs and hMSC-TERT, Stolzing and Scutt [32] and Ebert et al. [33] concluded that in "routine" cell culture MSCs have low antioxidant capacity. This conclusion based on the observation that modifications (selenium supplementation or temperature reduction, respectively) of the culture conditions used by these authors increased the activity of cells antioxidant system. As no comparison was performed against other cell type, a more appropriate conclusion should be that the basal antioxidant capacity of MSCs can be up regulated. A question that we have not tested, except for the depletion of GSx, in our primary low-passaged hMSCs isolated and expanded in alpha-MEM supplemented with FBS and at 37ºC.

The dependence of OS-resistance to high levels of intracellular GSx is explained because reduced glutathione plays a critical role in cellular defense against oxidative and nitrosative stress [35]. It is not only a substrate for GPX1 but also for other enzymes related to the management of OS. Together, it is able to directly scavenge reactive species. This dependence is not exclusive for hMSCs, since it has been shown that human T cell lymphocytes with high GSx levels readily eliminate ROS and are less susceptible to apoptosis [36].

A niche is a spatial microenvironment that allows tissue cells to function and also protects them. The redox status of the niche determines the intracellular levels of reactive species in parenchymal cells [34]. Stromal cells may scavenge extrinsic oxidative insults, e.g. inflammation. Hence, the therapeutic effects observed after the transplantation of MSCs into individuals with OS-related diseases might be attributed, among other mechanisms, to their potential to effectively scavenge exogenous ROS and RNS, once homed into the niche of damaged tissues. This hypothesis is supported by data here shown and also by

the observation that mice with experimental diseases that received MSCs showed a discrete but statistical significant lower ratio of reduced glutathione to oxidized glutathione [37] and a lower increase of disease-induced oxidative markers [38]. Further studies are needed to establish a causative relationship between the potential of hMSCs to efficiently scavenge reactive species and their contribution to tissue regeneration. Meanwhile, the correlation observed between OS management and therapeutic effects has, at least, three main implications when thinking on hMSCs as a tool for cell therapy: i) the concern that prolonged *ex vivo* expansion might impairs antioxidant defense ability of hMSCs, ii) the broadening of the putative therapeutic use of hMSCs. Now, they might be envisioned as a tool for cell therapy strategies aimed to treat patients with diseases which onset and progression is associated to OS; such as Diabetes, Cancer, Parkinson's, Huntington and Alzheimer diseases [35], and iii) the fact that hMSC pleiotropy is an outstanding feature because one single tool might limit tissue damage and promote its regeneration.

Acknowledgments

We thank Dr. Lisa Poppe (University Medical Center of Duke, USA) for providing the INS-1 clone 832/13 cells and Dr. Mafalda Maldonado (Universidad de Concepcion, Chile) for sharing the protocols to measure intracellular glutathione. We are in dept with Mrs. Patricia Luz for real-time RT-PCR standardization and with Mrs. Valeska Simon (Clinica Alemana-Universidad del Desarrollo, Chile) for helping us with flow cytometry analysis. We are very grateful to Dr. Yedy Israel (Universidad de Chile, Chile) and to Mrs. Michel Sparman (Oregon National Primate Research Center, USA) for English editing of this article. This work was supported by Universidad del Desarrollo grant number 4020203 (to A.V-P) and CONICYT fellowship 24071089 (to A.V-P). A.V-P was recipient of a PhD studentship from CONICYT.

Author Disclosure Statement

No competing financial interests exist.

References

[1] Wagers AJ and IL Weissman. (2004). Plasticity of adult stem cells. Cell 116:639-648.

[2] Conget PA and JJ Minguell. (1999). Phenotypical and functional properties of human bone marrow mesenchymal progenitor cells. J Cell Physiol 181:67-73.

[3] Pittenger MF, AM Mackay, SC Beck, RK Jaiswal, R Douglas, JD Mosca, MA Moorman, DW Simonetti, S Craig and DR Marshak. (1999). Multilineage potential of adult human mesenchymal stem cells. Science 284:143-147.

[4] Kotton DN, BY Ma, WV Cardoso, EA Sanderson, RS Summer, MC Williams, and A Fine. (2001). Bone marrow-derived cells as progenitors of lung alveolar epithelium. Development 128: 5181-5188.

[5] Lee KD, TK Kuo, J Whang-Peng, YF Chung, CT Lin, SH Chou, JR Chen, YP Chen and OK Lee. (2004). In vitro hepatic differentiation of human mesenchymal stem cells. Hepatology 40:1275-1284.

[6] Sanchez-Ramos J, S Song, F Cardozo-Pelaez, C Hazzi, T Stedeford, A Willing, TB Freeman, S Saporta, W Janssen, N Patel, DR Cooper and PR Sanberg. (2000). Adult bone marrow stromal cells differentiate into neural cells in vitro. Exp Neurol 164:247-256.

[7] Moriscot, C, F Fraipont, MJ Richard, M Marchand, P Savatier, D Bosco, M Favrot and P Benhamou. (2005). Human bone marrow mesenchymal stem cells can express insulin and key transcription factors of the endocrine pancreas

developmental pathway upon genetic and/or microenvironmental manipulation in vitro. Stem Cells 23:594-604.

[8] Le Blanc K and O Ringden. (2005). Immunobiology of human mesenchymal stem cells and future use in hematopoietic stem cell transplantation. Am Soc Blood Marrow Trans 11:321-334.

[9] Ryan JM, FP Barry, JM Murphy and BP Mahon. (2005). Mesenchymal stem cells avoid allogeneic rejection. J Inflamm (Lond) 2:8.

[10] Horwitz EM, PL Gordon, WK Koo, JC Marx, MD Neel, RY McNall, L Muul and T Hofmann. (2002). Isolated allogeneic bone marrow-derived mesenchymal cells engraft and stimulate growth in children with osteogenesis imperfecta: Implications for cell therapy of bone. Proc Natl Acad Sci (USA) 99:8932-8937.

[11] Conget P, F Rodriguez, S Kramer, C Allers, V Simon, F Palisson, S Gonzalez and MJ Yubero. (2010). Replenishment of type VII collagen and reepithelialization of chronically ulcerated skin after intradermal administration of allogeneic Mesenchymal Stem Cells in a patient with Recessive Dystrophic Epidermolysis Bullosa. Cytotherapy: in press.

[12] Le Blanc K, I Rasmusson, B Sundberg, C Gotherstrom, M Hassan, M Uzunel and O Ringden. (2004). Treatment of severe acute graft versus-host disease with third party haploidentical mesenchymal stem cells. Lancet 363:1439-1441.

[13] Chen SL, WW Fang, F Ye, YH Liu, J Qian, SJ Shan, JJ Zhang, RZ Chunhua, LM Liao, S Lin and JP Sun. (2004). Effect on left ventricular function of intracoronary transplantation of autologous bone marrow mesenchymal stem cell in patients with acute myocardial infarction. Am J Cardiol 94:92-95.

[14] Kurozumi K, K Nakamura, T Tamiya, Y Kawano, K Ishii, M Kobune, S Hirai, H Uchida, K Sasaki, Y Ito, K Kato, O Honmou, K Houkin, I Date and H Hamada.

(2005). Mesenchymal stem cells that produce neurotrophic factors reduce ischemic damage in the rat middle cerebral artery occlusion model. Mol Ther 11:96-104.

[15] Lee RH, MJ Seo, RL Reger, JL Apees, AA Pulin, SD Olson and DJ Prockop. (2006). Multipotent stromal cells from human marrow home to and promote repair of pancreatic islets and renal glomeruli in diabetic NOD/scid mice. Proc Natl Acad Sci (USA) 103:17438-17443.

[16] Ezquer FE, ME Ezquer, DB Parrau, D Carpio, AJ Yañez and PA Conget. (2008). Systemic Administration of Multipotent Mesenchymal Stromal Cells Reverts Hyperglycemia and Prevents Nephropathy in Type 1 Diabetic Mice. Biol Blood Marrow Transpl 14:631-640.

[17] Caplan AI and JE Dennis. (2006). Mesenchymal stem cells as trophic mediators. J Cell Biochem 98:1076-1084.

[18] Halliwell B and M Whiteman. (2004). Measuring reactive species and oxidative damage in vivo and in cell culture: how should you do it and what do the results mean? Br J Pharmacol 142:231-255.

[19] Chen MF, CT Lin, WC Chen, CT Yang, CC Chen, SK Liao, JM Liu, CH Lu and KD Lee. (2006). The sensitivity of human mesenchymal stem cells to ionizing radiation. Int. J Radiat Oncol Biol Phys 66:244-253.

[20] Tran VV, G Chen, CB Newgard and HE Hohmeier. (2003). Discrete and complementary mechanisms of protection of beta-cells against cytokine-induced and oxidative damage achieved by bcl-2 overexpression and a cytokine selection strategy. Diabetes 52:1423-1432.

[21] Hohmeier HE, H Mulder, G Chen, R Henkel-Rieger, M Prentki and CB Newgard. (2000). Isolation of INS-1-derived cell lines with robust ATP-sensitive K^+ channel-dependent and -independent glucose-stimulated insulin secretion. Diabetes 49:424-430.

[22] Kaliberova LN, DL Della Manna, V Krendelchtchikova, ME Black, DJ Buchsbaum and SA Kaliberova. (2008) Molecular chemotherapy of pancreatic cancer using novel mutant bacterial cytosine deaminase gene. Mol Cancer Ther 7:2845-2854.

[23] Tajouri L, AS Mellick, KJ Ashton, AE Tannenberg, RM Nagra, WW Tourtellotte and LR Griffiths. (2003). Quantitative and qualitative changes in gene expression patterns characterize the activity of plaques in multiple sclerosis. Brain Res Mol 119:170-183.

[24] Hamanishi T, H Furuta, H Kato, A Doi, M Tamai, H Shimomura, S Sakagashira, M Nishi, H Sasaki, T Sanke and K Nanjo. (2004). Functional variants in the glutathione peroxidase-1 (GPx-1) gene are associated with increased intima-media thickness of carotid arteries and risk of macrovascular diseases in japanese type 2 diabetic patients. Diabetes 53:2455-2460.

[25] Millington-Ward S, C Allers, G Tuohy, P Conget, D Allen, HP McMahon, PF Kenna, P Humphries and GJ Farrar. (2002). Validation in mesenchymal progenitor cells of a mutation-independent ex vivo approach to gene therapy for osteogenesis imperfecta. Hum Mol Genet 11:2201-2206.

[26] Schmittgen TD and KJ Livak. (2008). Analyzing real-time PCR data by the comparative C(T) method. Nat Protoc 3:1101-1108.

[27] Janjic D and CB Wollheim. (1992). Effect of 2-mercaptoethanol on glutathione levels, cystine uptake and insulin secretion in insulin-secreting cells. Eur J Biochem 210:297-304.

[28] Tietze F. (1969). Enzymic method for quantitative determination of nanogram amounts of total and oxidized glutathione: applications to mammalian blood and other tissues. Anal Biochem 27:502-522.

[29] Baker MA, GJ Cerniglia and A Zaman. (1990). Microtiter plate assay for the measurement of glutathione and glutathione disulfide in large numbers of biological samples. Anal Biochem 190:360-365.

[30] Salmon AB, VI Perez, A Bokov, A Jemigan, G Kim, H Zhao, RH Levine and A Richardson. (2009). Lack of methionine sulfoxide reductase A in mice increases sensitivity to oxidative stress but does not diminish life span. FASEB J 23:3601-3608.

[31] Silva WA, DT Covas, RA Panepucci, R Proto-Siqueira, JL Siufi, DL Zanette, AR Santos and MA Zago. (2003). The profile of gene expression of human marrow mesenchymal stem cells. Stem Cells 21:61-669.

[32] Stolzing A and A Scutt. (2006). Effect of reduced culture temperature on antioxidant defenses of mesenchymal stem cells. Free Radic Biol Med 41:326-338.

[33] Ebert R, M Ulmer, S Zeck, J Meissner-Weigl, D Schneider, H Stopper, N Schupp, M Kassem and F Jacob. (2006). Selenium supplementation restores the antioxidative capacity and prevents cell damage in bone marrow stromal cells in vitro. Stem Cells 24:1226-1235.

[34] Naka K, T Muraguchi, T Hoshii and A Hirao. (2008). Regulation of reactive oxygen species and genomic stability in hematopoietic stem cells. Antioxid Redox Signal 10:1883-1894.

[35] Franco R, OJ Schoneveld, A Pappa and MI Panayiotidis. (2007). The central role of glutathione in the pathophysiology of human diseases. Arch Physiol Biochem 113:234-258.

[36] Larbi A, F Cabreiro, H Zelba, S Marthandan, E Combet, B Friguet. I Petropoulos, Y Barnett and G Pawelec. (2010). Reduced oxygen tension results in reduced human T cell proliferation and increased intracellular oxidative damage and susceptibility to apoptosis upon activation. Free Rad Biol Med 48:26-34.

[37] Kuo TK, SP Hung, CH Chuang, CT Chen, YR Shih, SC Fang, VW Yang and OK Lee. (2008). Stem cell therapy for liver disease: parameters governing the success of using bone marrow mesenchymal stem cells. Gastroenterology 134:2111-2121.

[38] Lanza C, S Morando, A Voci, L Canesi, MC Principato, LD Serpero, G Mancardi, A Uccelli and L Vergani. (2009). Neuroprotective mesenchymal stem cells are endowed with a potent antioxidant effect in vivo. J Neurochem 110:1674-1684.

Table 1. Specific primers for real time RT-PCR.

Gene	Nº GenBank access	Sense (5'→3')	Antisense (5'→3')	Amplicon		Reference
				Tm (ºC)	size (bp)	
hSOD1	NM_000454	GGT CCT CAC TTT AAT CCT CTA T	CAT CTT TGT CAG CAG TCA CAT T	83	96	[23]
hSOD2	S77127	TGA CAA GTT TAA GGA GAA GC	GAA TAA GGC CTG TTG TTC C	85	148	----
hCAT	NM_001752	TTA ATC CAT TCG ATC TCA CC	GGC GGT GAG TGT CAG GAT AG	87	210	----
hGPX1	NM_000581	CGC CAC CGC GCT TAT GAC CG	GCA GCA CTG CAA CTG CCA AGC AG	93	238	[24]
GADPH	AF261085	CAG CCT CAA GAT CAT CAG CA	CAT GAG TCC TTC CAC GAT AC	85	100	[25]

T_m adjusted to salt concentration of the LightCycler-DNA Master SYBR Green I kit (200 mM K^+, 200 mM Na^+, 3 mM Mg^{+2}) using BioMath-T_m calculations for oligos software (http://www.promega.com/biomath/calc11.htm#disc).

Table 2. High resistance of hMSCs to OS-induced death.

	H_2O_2	SNAP	SIN-1
	LC_{50} (mM)		
INS-1 (n=3)	0.31 ± 0.01	0.09 ± 0.03	1.42 ± 0.35
hMSCs (n=7)	2.10 ± 0.56*	9.14 ± 1.01**	4.28 ± 0.13*
hFibs (n=6)	0.80 ± 0.11*	7.63 ± 0.92**	3.44 ± 0.29*

LC_{50}: concentration at which survives 50% of the cells.

Numbers in parentheses indicate the number of samples analyzed.

Data correspond to mean ± standard error.

Statistical analysis versus INS-1 cells: (*) $p < 0.05$, (**) $p < 0.0005$

Table 3. Gene expression of *SOD1, SOD2, CAT* and *GPX1* in hMSCs.

	SOD1	***SOD2***	***CAT***	***GPX1***
	relative gene expression			
hMSCs (n=3)	1.11 ± 0.16	0.60 ± 0.04	0.74 ± 0.06	1.06 ± 0.11
hFibs (n=3)	0.75 ± 0.02	0.78 ± 0.10	0.70 ± 0.05	0.88 ± 0.06

Relative gene expression: Ct gene of interest/Ct *GAPDH*

Numbers in parentheses indicate the number of samples analyzed.

Data correspond to mean ± standard error.

Statistical analysis versus hFibs: no statistical significance.

Figure Legends

Figure 1. Raw data of cytotoxicity assay and LC_{50} interpolation. INS-1 cells, hMSCs and hFibs were cultured in the presence or not of different concentrations of ROS and/or RNS sources. Eighteen hours later, adherent cells were stained with crystal violet and the percentage of cells that survived (viability) in each condition was determined. Data were plotted and lineal regression analysis was performed. LC_{50} value corresponds to the concentration at which viability is 50%.

Figure 2. Low intracellular levels of reactive species in hMSCs exposed to OS. INS-1 cells, hMSCs and hFibs were incubated with or without 0.75 mM SIN-1 for 1 hour. Levels of intracellular peroxide and peroxynitrite were assessed by flow cytometry after staining with DHR. Data shown correspond to the ratio between NFI of cells exposed to SIN-1 and NFI of cells unexposed. Numbers in parentheses indicate the number of samples analyzed. ns = no statistical significance.

Figure 3. Gene expression of *SOD1, SOD2, CAT* and *GPX1* in hMSCs. Total RNA isolated from hMSCs was amplified with specific primers for referred genes. Real-time PCR products were analyzed according to their melting point. Positive control = RNA isolated from HeLa cells. Negative control = reaction without template. Data is representative of 3 different samples.

Figure 4. Enzymatic activity of SOD, CAT and GPX1 in hMSCs.

INS-1 cells, hMSCs and hFibs were collected and the enzymatic activity of SOD (A), CAT (B) and GPX1 (C) were assessed with commercial kits. Data obtained were standardized against total protein and shown as U/mg for SOD and nmol/min/mg for CAT and for GPX1.

Numbers in parentheses indicate the number of samples analyzed. ns = no statistical significance.

Figure 5. High levels of GSx in hMSCs. INS-1 cells, hMSCs and hFibs were collected and intracellular GSx was assessed by the method described by Tietze [27] and adjusted for microplates [28]. Numbers in parentheses indicate the number of samples analyzed. ns = no statistical significance.

Figure 6. High resistance of hMSCs to OS-induced death depends on GSx availability. Cytotoxicity assays were performed with hMSCs (n = 7) and INS-1 cells (n = 3) cultured in standard conditions and with hMSCs exposed to BSO and DEM (GSx-depleted hMSCs, n = 3). Exposure of hMSCs to these inhibitors resulted in a depletion of GSx higher 80% that last for up to 11 hours. ns = no statistical significance.

Figure 1

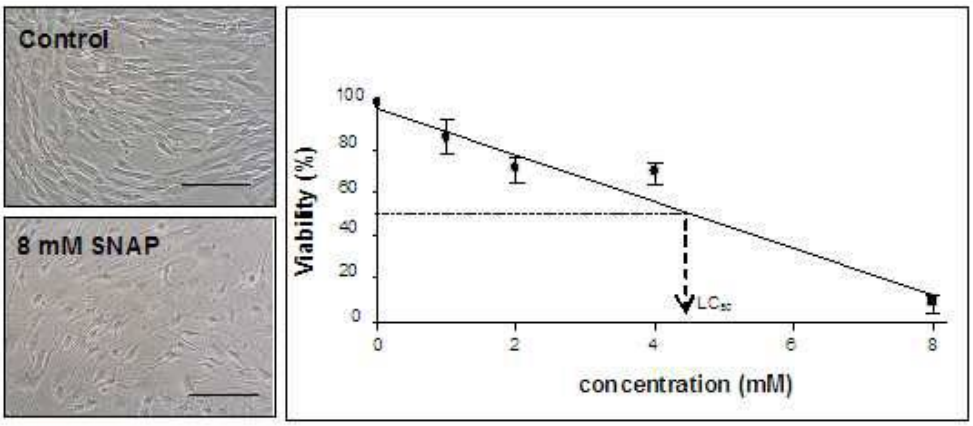

194x97mm (72 x 72 DPI)

Figure 2

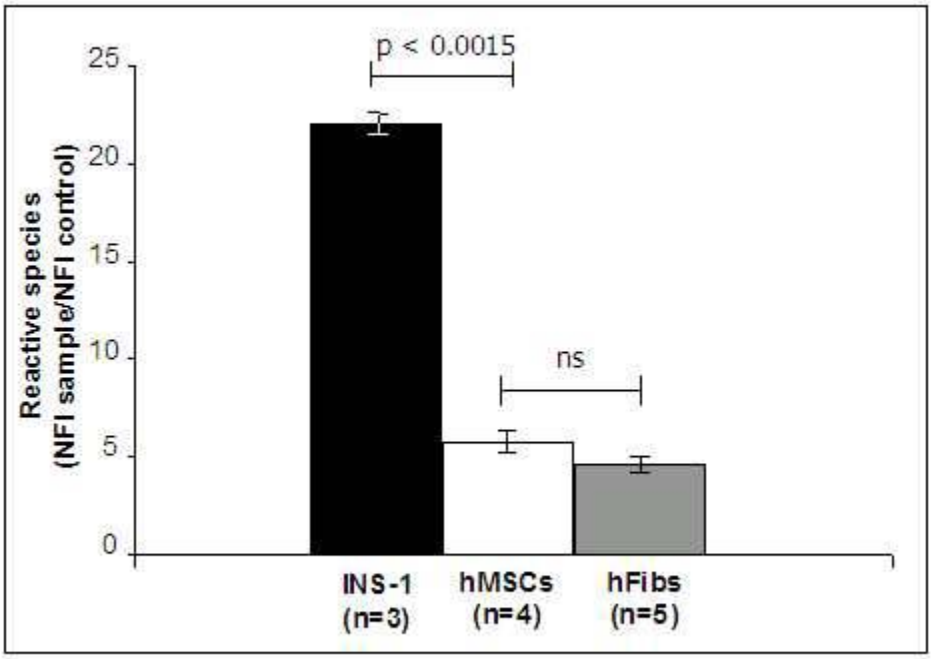

169x146mm (72 x 72 DPI)

Figure 3

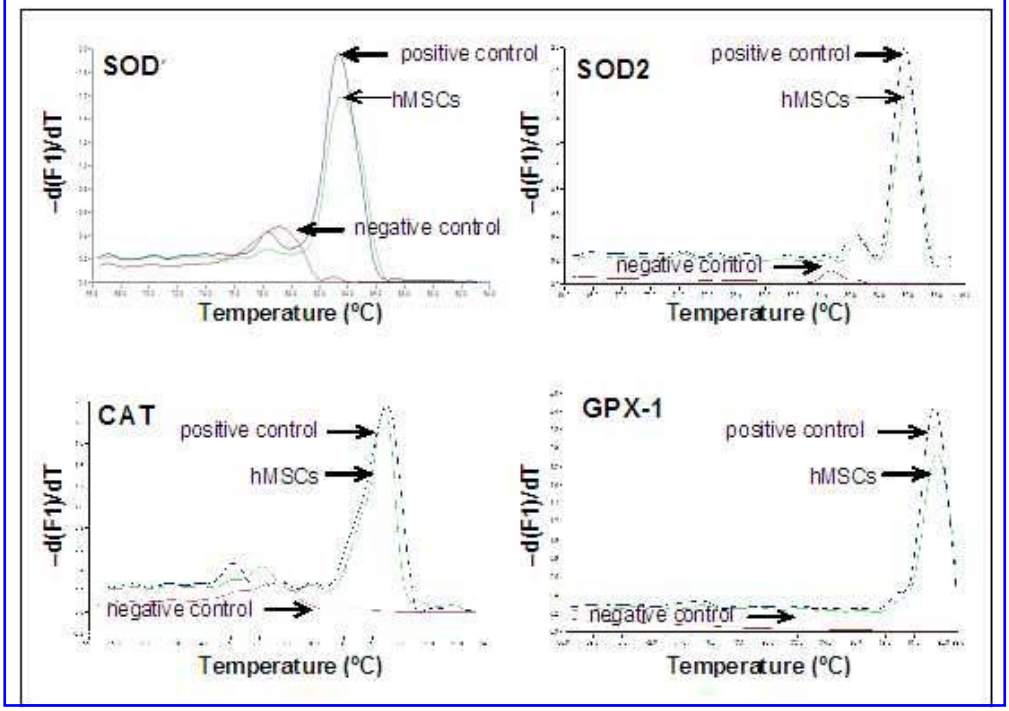

196x154mm (72 x 72 DPI)

Figure 4

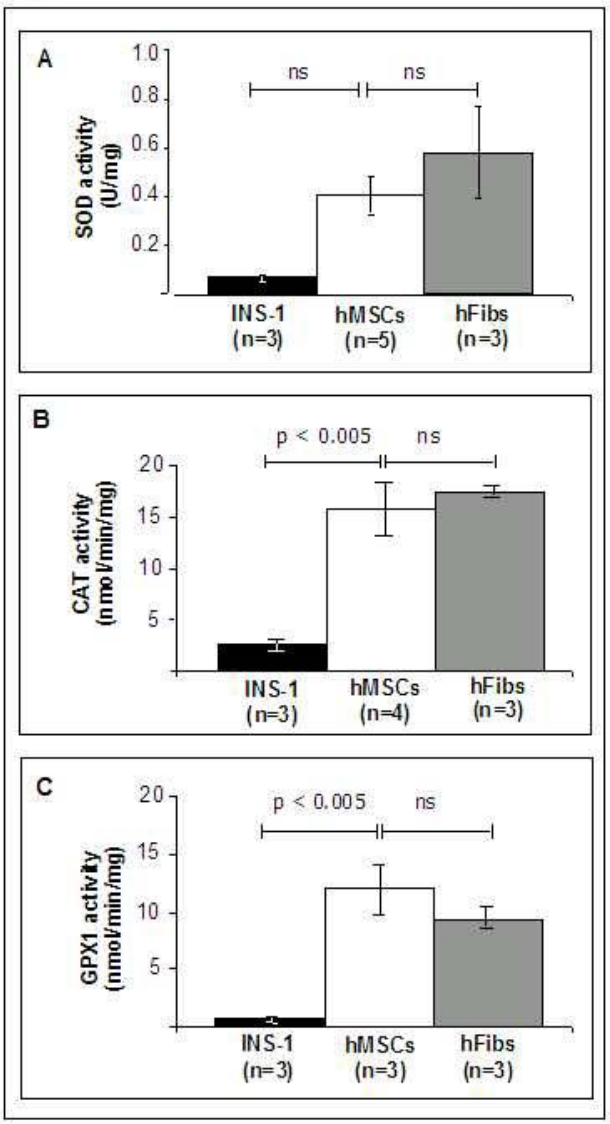

138x253mm (72 x 72 DPI)

Figure 5

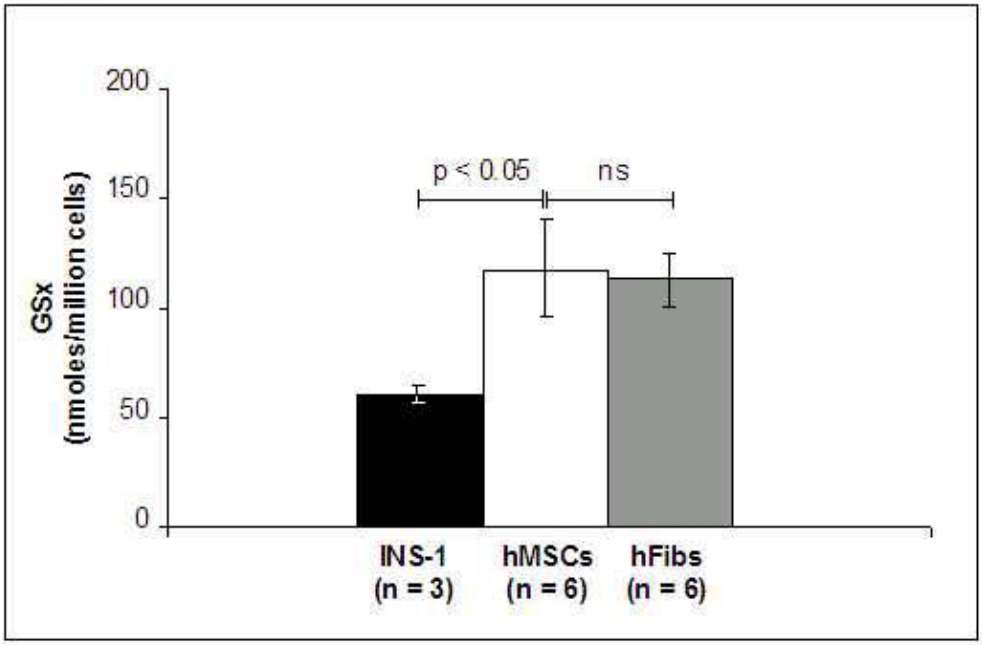

184x131mm (72 x 72 DPI)

Figure 6

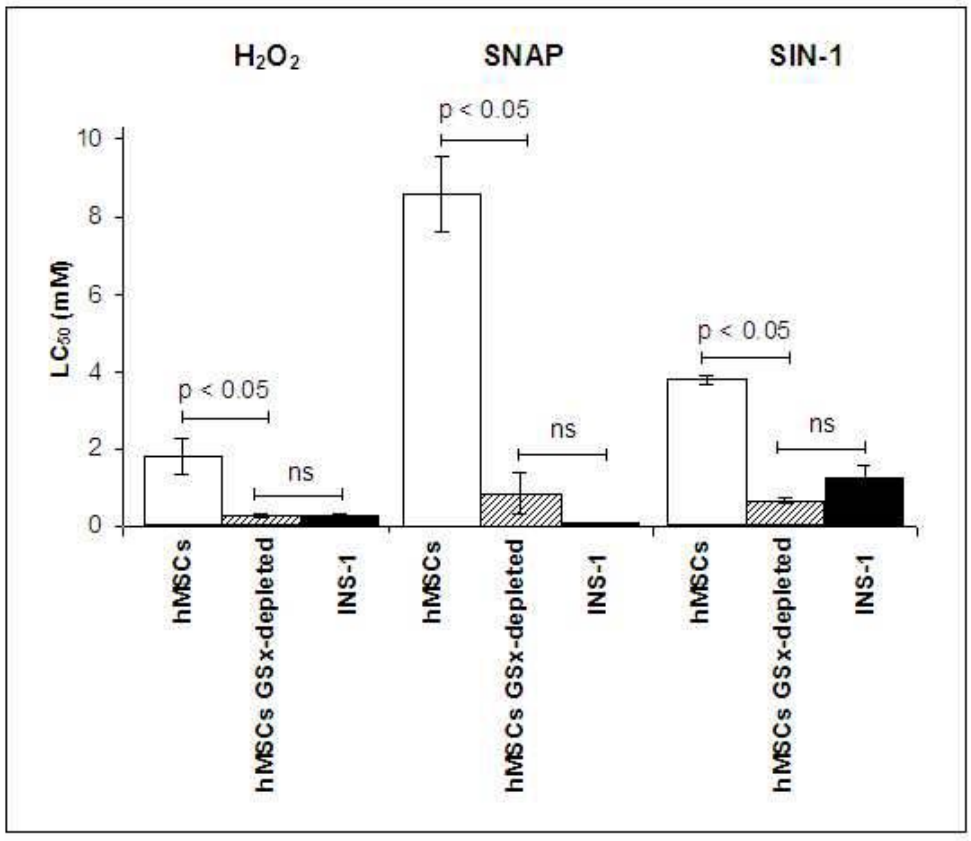

196x185mm (72 x 72 DPI)